

# JOM

A publication of The Minerals, Metals & Materials Society

## **The Oxidation and Protection of Gamma Titanium Aluminides**

---

Michael P. Brady, William J. Brindley, James L. Smialek, and Ivan E. Locci

# The Oxidation and Protection of Gamma Titanium Aluminides

Michael P. Brady, William J. Brindley, James L. Smialek, and Ivan E. Locci

**Authors' Note:** All compositions are in atomic percent.

*The excellent density-specific properties of the gamma class of titanium aluminides make them attractive for intermediate-temperature (600–850°C) aerospace applications. The oxidation and embrittlement resistance of these alloys is superior to that of the  $\alpha_1$  and orthorhombic classes of titanium aluminides. However, since gamma alloys form an intermixed  $Al_2O_3/TiO_2$  scale in air rather than the desired continuous  $Al_2O_3$  scale, oxidation resistance is inadequate at the high end of this temperature range (i.e., greater than 750–800°C). For applications at such temperatures, an oxidation-resistant coating will be needed; however, a major drawback of the oxidation-resistant coatings currently available is severe degradation in fatigue life by the coating. A new class of oxidation-resistant coatings based in the Ti-Al-Cr system offers the potential for improved fatigue life.*

## INTRODUCTION

Titanium aluminides based on the  $\gamma$  (TiAl) phase offer the potential for component weight savings of up to 50 percent over conventional superalloys in 600–850°C aerospace applications.<sup>1,2</sup> Extensive development efforts during the past ten years have led to the identification of engineering  $\gamma$  alloys such as Ti-48Al-2Cr-2Nb,<sup>3</sup> which offer a balance of room-temperature mechanical properties (1–4% elongation, 10–20 MPa·m<sup>1/2</sup> fracture toughness) and high-temperature strength retention (300–500 MPa tensile strength at 800°C).<sup>1</sup> These alloys are generally based on Ti-(45–48)Al and contain 3–15 volume percent  $\alpha_2$  (Ti<sub>3</sub>Al) as a second phase (Figure 1).<sup>1,2</sup>

The  $\gamma$  class of titanium aluminides also offers oxidation and interstitial (oxygen, nitrogen) embrittlement resistance superior to that of the  $\alpha_1$  and orthorhombic (Ti<sub>2</sub>AlNb) classes of titanium aluminides. However, environmental durability is still a concern, especially at temperatures above 750–800°C in air.

In this article, the fundamental aspects governing the oxidation behavior of gamma titanium aluminides are reviewed. The controversy regarding the Ti-Al-O phase diagram, the recently gained understanding of the detrimental role played by nitrogen during oxidation in air, and the oxidation and embrittlement behavior of engineering  $\gamma$

alloys are discussed. The development of oxidation-resistant coatings for engineering  $\gamma$  alloys is also reviewed, with a focus on the promising recent work in the Ti-Al-Cr system.

## FUNDAMENTALS OF GAMMA TITANIUM ALUMINIDE OXIDATION

The goal during the oxidation of  $\gamma$  titanium aluminides (and aluminides in general) is to form a continuous  $Al_2O_3$  ( $\alpha$ ) scale. Alumina ( $Al_2O_3$ ) scales, by virtue of their extremely slow, parabolic rate of growth, are protective at temperatures in excess of 1,200°C. Unfortunately, during the oxidation of  $\gamma$  alloys in air, an intermixed  $Al_2O_3/TiO_2$  scale rather than a continuous  $Al_2O_3$  scale is formed.<sup>5–10</sup> Intermixed  $Al_2O_3/TiO_2$  scales are generally protective only to about 750–800°C. They are less protective than continuous  $Al_2O_3$  scales because TiO<sub>2</sub> has a much higher rate of growth than  $Al_2O_3$ . Titania (TiO<sub>2</sub>) may also act as a short-circuit transport path, resulting in interstitial oxygen/nitrogen dissolution into the alloy during elevated-temperature exposure in air. This can embrittle the alloy and degrade mechanical properties, in particular, fatigue life.

## Thermodynamics and the Ti-Al-O System

A prerequisite for continuous  $Al_2O_3$  scale formation during oxidation is that  $Al_2O_3$  must be the most stable oxide on the alloy. However, the most stable oxide of titanium, usually TiO (depending upon temperature), is nearly as stable as  $Al_2O_3$ . The activity of aluminum in the Ti-Al system exhibits a large negative deviation from ideality.<sup>11–14</sup> Therefore, the activities of aluminum and titanium in a given alloy determine whether TiO

or  $Al_2O_3$  is the stable oxide for that particular composition. If TiO is more stable than  $Al_2O_3$ , a titanium-based oxide scale is formed. Such scales predominately contain TiO<sub>2</sub> instead of TiO because of kinetic factors involved (discontinuous  $Al_2O_3$  particles may also be present in the scale).

Thermodynamic calculations by Luthra (800°C)<sup>15</sup> and Rahmel et al. (700°C, 900°C, and 1,100°C)<sup>16</sup> indicated that TiO was stable on binary Ti-Al alloys containing less than about 50% aluminum (Figure 2). Thus, it was proposed that  $\gamma$  alloys could not form a continuous  $Al_2O_3$  scale because  $Al_2O_3$  was not the most thermodynamically stable oxide on the alloy. However, recent experimental evidence shows that  $Al_2O_3$  is more stable than TiO on Ti-Al alloys containing as little as approximately 5–25% aluminum (Figure 3).<sup>17–20</sup>

Li et al.<sup>17</sup> and Becker et al.<sup>6</sup> have explained the differences between the thermodynamically calculated Ti-Al-O phase diagram (Figure 2) and the experimentally determined Ti-Al-O phase diagram (Figure 3). They propose that oxygen solubility in the metal phases (in particular,  $\alpha_1$  and  $\gamma$ ), which was neglected in the thermodynamic calculations, plays a critical role in stabilizing  $Al_2O_3$ . Calculations by Li et al.<sup>17</sup> suggest that when oxygen solubility in these phases is considered, a thermodynamically calculated Ti-Al-O phase diagram can match the experimentally determined Ti-Al-O phase diagram (Figure 3).

There has also been recent experimental evidence that one or more new ternary Ti<sub>x</sub>Al<sub>y</sub>O<sub>z</sub> phases, with an approximate composition of Ti-(25–35)Al-(15–20)O, may exist.<sup>21–25</sup> The existence of such phase(s), with unknown thermodynamic properties, could also account for the discrepancies between the thermodynamically calculated and experimentally determined Ti-Al-O phase diagrams.<sup>23</sup> While very recent data suggest that these Ti<sub>x</sub>Al<sub>y</sub>O<sub>z</sub> phases may be metastable,<sup>26</sup> the key point is that the experimental Ti-Al-O phase diagram studies clearly indicate that  $Al_2O_3$  stability is not a barrier to  $\gamma$  alloys oxidizing to establish a continuous  $Al_2O_3$  scale.

## The Nitrogen Effect

Binary  $\gamma$  alloys form a continuous  $Al_2O_3$  scale at temperatures up to 1,000°C in

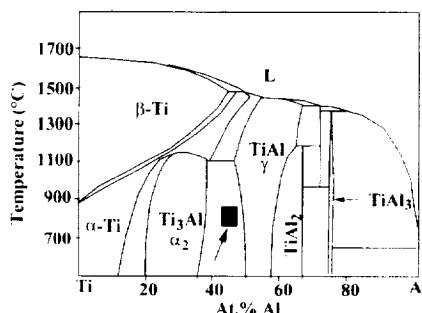


Figure 1. Binary Ti-Al phase diagram.<sup>4</sup>

pure oxygen, but do not form a continuous alumina scale in air.<sup>27</sup> Approximately 60–70% aluminum is needed for binary Ti–Al alloys to form a continuous  $\text{Al}_2\text{O}_3$  scale in air, while only about 47–49% aluminum is needed in pure oxygen.<sup>5</sup> The poor oxidation behavior of  $\gamma$  alloys in air, as compared with pure oxygen, is commonly referred to as “the nitrogen effect.” The nitrogen effect is significant because many of the engineering  $\gamma$  alloys, like the binary  $\gamma$  alloys, contain sufficient aluminum for continuous  $\text{Al}_2\text{O}_3$  scale formation in oxygen but not in air.

The nitrogen effect has recently been the subject of intense, fundamental-oriented studies geared toward developing a mechanistic understanding of this phenomenon.<sup>5,6,28–30</sup> Dettenwanger and Rakowski et al. proposed that the inability of binary  $\gamma$  alloys to establish a continuous  $\text{Al}_2\text{O}_3$  scale from 800–900°C in air is related to the formation of TiN during the initial stages of oxidation.<sup>28,29</sup> Cross-section transmission electron mi-

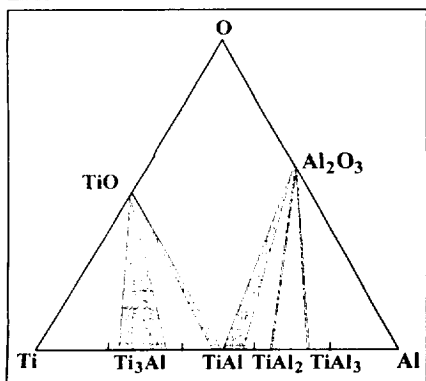


Figure 2. A schematic partial Ti–Al–O phase diagram obtained from thermodynamic calculations (based on Luthra<sup>15</sup> and Rahmel et al.<sup>16</sup>). The two-phase fields with TiO and  $\text{Al}_2\text{O}_3$  are highlighted in gray and show  $\gamma$  in equilibrium with both  $\text{Al}_2\text{O}_3$  and TiO.

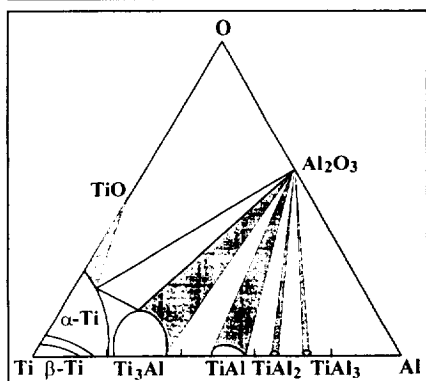


Figure 3. A schematic partial Ti–Al–O phase diagram obtained from experimental studies (based on References 17–20). The two-phase fields with TiO and  $\text{Al}_2\text{O}_3$  are highlighted in gray and show that both  $\gamma$  and  $\alpha_2$  are in equilibrium with  $\text{Al}_2\text{O}_3$ . Note that although the cited studies agree that  $\text{Al}_2\text{O}_3$  is the stable oxide for Ti–( $<<50$ )Al, the details of the  $\text{Al}_2\text{O}_3$ /TiO stability changeover vary somewhat from study to study.

croscopy (TEM) analysis of the scale formed on Ti–50Al after one hour at 900°C in air revealed an alternating sequence of TiN and  $\text{Al}_2\text{O}_3$  at the metal/scale interface.<sup>28,29</sup> The presence of TiN in this layer was postulated to interrupt the establishment of a continuous  $\text{Al}_2\text{O}_3$  scale (Figure 4).<sup>28,29</sup> As oxidation proceeds, the TiN is subsequently oxidized to form  $\text{TiO}_2$ .<sup>29</sup> This process results in the formation of an intermixed  $\text{Al}_2\text{O}_3$ / $\text{TiO}_2$  scale rather than a continuous  $\text{Al}_2\text{O}_3$  scale (Figure 4).<sup>29</sup>

Although further experimental confirmation is needed, the Dettenwanger and Rakowski et al. mechanism provides a very plausible explanation for the nitrogen effect. Regardless of the exact mechanistic details, the nitrogen effect appears to be the main barrier to continuous  $\text{Al}_2\text{O}_3$  scale formation by  $\gamma$  alloys in air.

### Oxidation and Embrittlement of Engineering $\gamma$ Titanium Aluminides

Ternary and higher order alloying additions can reduce the rate of oxidation of  $\gamma$  alloys.<sup>6,7,9,10, 27, 31–39</sup> Of particular benefit are small (1–4%) ternary additions of tungsten, niobium, and tantalum.<sup>9,27,33–37,39</sup> When combined with quaternary additions of 1–2% chromium or manganese, further improvement in oxidation resistance is gained.<sup>34,37</sup> However, it is important to stress that these small alloying additions do not result in continuous  $\text{Al}_2\text{O}_3$  scale formation. Rather, a complex intermixed  $\text{Al}_2\text{O}_3$ / $\text{TiO}_2$  scale is still formed, but the rate of growth of this scale is reduced.

The mechanisms by which these small alloying additions slow the rate of oxidation of  $\gamma$  alloys are not well understood.<sup>10</sup> Proposed explanations include the reduced growth rate of  $\text{TiO}_2$  by doping,<sup>27</sup> an increase in Al/Ti activity ratio to favor  $\text{Al}_2\text{O}_3$  scale formation,<sup>6,27,34</sup> and a reduction in alloy oxygen solubility to prevent internal oxidation.<sup>9,39</sup> However, further experimental examination of the influence of these mechanisms on the oxidation behavior of  $\gamma$  alloys is needed, particularly in the 600–850°C application temperature range.

Based on the following data and the data available in the literature,<sup>32,37,38,40,41</sup> engineering  $\gamma$  alloys exhibit acceptable oxidation rates up to about 750–800°C in air. Figure 5<sup>41</sup> shows oxidation data for several engineering  $\gamma$  alloys of current interest: Ti–48Al–2Cr–2Nb, Ti–46.5Al–3Nb–2Cr–0.2W (K-5),<sup>42</sup> and Ti–46Al–5Nb–1W (Alloy 7)<sup>43</sup> at 800°C in air. At regular intervals, the samples were removed from the test furnace at temperature, air-cooled, weighed, and returned to the test furnace at temperature (i.e., interrupted weight-gain test). Therefore, interrupted weight-gain exposures involve both an isothermal and cyclic temperature component.

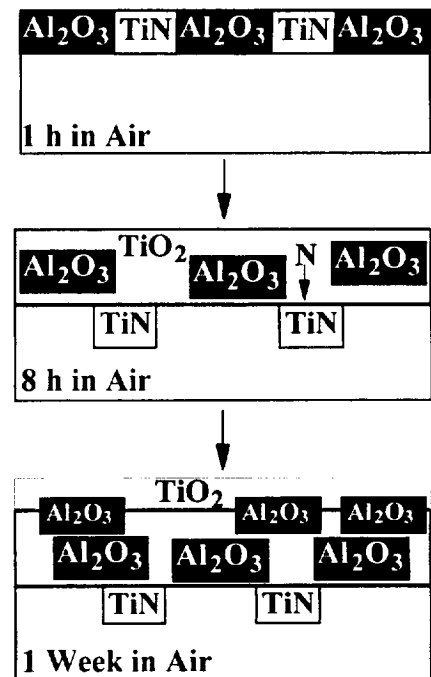


Figure 4. Portions of the Rakowski et al. schematic mechanism of the nitrogen effect for binary  $\gamma$  alloys at 800–900°C in air (a description is provided only for the external scale).<sup>29</sup>

The Ti–48Al–2Cr–2Nb alloy samples oxidized at a relatively rapid rate, with one of the two samples suffering from significant scale spallation (weight loss) after about 500 hours at 800°C in air (Figure 5). The K-5 and Alloy 7  $\gamma$  alloys exhibited low rates of oxidation up to 1,000 hours at 800°C in air. The superior oxidation resistance of K-5 and Alloy 7 is attributable to the presence of tungsten and a higher level of niobium in these alloys. However, the oxidation kinetics for K-5 and Alloy 7 were strongly linear in character beyond 500 hours, which suggests a possible degradation in the protectiveness of the scale.

The scale formed on Ti–48Al–2Cr–2Nb after 9,000 hours of isothermal oxidation at 704°C in air is shown in Figure 6 (after Locci et al.).<sup>40</sup> Despite the very long-term exposure, the scale is only about 15  $\mu\text{m}$  thick, an acceptable rate of oxidation for many applications. From the gas/scale interface inward, the microstructure consisted of  $\text{TiO}_2$ / $\text{Al}_2\text{O}_3$ -rich (not continuous)/intermixed  $\text{Al}_2\text{O}_3$ + $\text{TiO}_2$ /TiN/TiAl<sub>2</sub>/bulk alloy. (The identification of TiN and TiAl<sub>2</sub> were based solely on composition data obtained by wavelength dispersive analysis.)

The outer-scale microstructure formed on Ti–48Al–2Cr–2Nb after 9,000 hours at 704°C in air (Figure 6) is qualitatively similar to that reported for binary  $\gamma$  alloys after short-term, high-temperature exposures (less than 1,000 hours at 900–1,000°C) in air.<sup>5,6,10</sup> (Little information is available on the scales formed on binary  $\gamma$  alloys after long-term, low-temperature exposures such as is available for Ti-

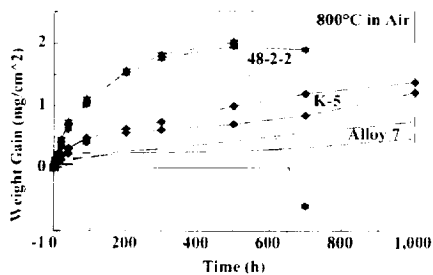


Figure 5. Interrupted weight gain oxidation data for Ti-48Al-2Cr-2Nb (48-2-2), Ti-46.5Al-3Nb-2Cr-0.2W (K-5), and Ti-46Al-5Nb-1W (Alloy 7) at 800°C in air.<sup>41</sup>

48Al-2Cr-2Nb.) However, the inner-scale microstructure is markedly different. In binary  $\gamma$  alloys, discrete TiN particles<sup>28,29</sup> as well as an embrittled zone of aluminum-depleted, oxygen-rich metal phase(s)<sup>21,25,44</sup> are formed at the metal/scale interface. In Ti-48Al-2Cr-2Nb, a continuous layer of TiN is formed at the metal/scale interface (Figure 6).<sup>40</sup> The depletion of titanium to form the TiN layer effectively enriches the alloy in aluminum, which then results in the formation of TiAl<sub>2</sub> just below the TiN layer (Figure 6).

The formation of this TiAl<sub>2</sub> layer is postulated to be beneficial from an environmental durability viewpoint. First, as oxidation proceeds, the TiAl<sub>2</sub> layer would primarily be oxidized to form Al<sub>2</sub>O<sub>3</sub>. Second, because of its high aluminum content, TiAl<sub>2</sub> is expected to have a low permeability to oxygen and nitrogen. Therefore, the TiAl<sub>2</sub> layer would aid in resisting interstitial oxygen/nitrogen penetration and embrittlement. A possible concern, however, is a degradation in mechanical properties, especially fatigue life, because the TiN and TiAl<sub>2</sub> phases are themselves extremely brittle.

The scale formed by Ti-48Al-2Cr-2Nb provides adequate oxidation resistance up to 750–800°C in air. However, it is not clear if it is a sufficient barrier to interstitial oxygen/nitrogen penetration into the alloy. Significant penetration of oxygen or nitrogen could lead to interstitial embrittlement, as is observed in the  $\alpha_2$  and orthorhombic titanium aluminides,<sup>36,45,46</sup> and a subsequent degradation of mechanical properties.

Electron microprobe analysis of the Ti-48Al-2Cr-2Nb sample oxidized for 9,000 hours at 704°C in air showed no evidence of oxygen/nitrogen penetration into the alloy ahead of the metal/scale interface.<sup>40</sup> Cross-section microhardness evaluation of Ti-48Al-2Cr-2Nb oxidized for 700 hours at 800°C in air (Figure 7) also showed little evidence of interstitial hardening ahead of the metal/scale interface.<sup>41</sup> Similar results were obtained for K-5 and Alloy 7.<sup>41</sup> By comparison, the orthorhombic-based alloy Ti-22Al-20Nb-2Ta-1Mo, which is more oxidation resistant than Ti-48Al-2Cr-2Nb at 800°C in air (Figure 8), suffers from

extensive interstitial embrittlement ahead of the metal/scale interface (Figure 7).<sup>47</sup> This suggests that the oxidation rate of titanium aluminides does not necessarily correlate with susceptibility to interstitial embrittlement<sup>47</sup> and that engineering  $\gamma$  alloys exhibit superior resistance to interstitial penetration as compared to  $\alpha_2$  and orthorhombic alloys.<sup>41,47</sup>

However, electron microprobe and microhardness evaluations are only sensitive to interstitial penetration beyond about 5  $\mu$ m from the metal/scale interface. Fatigue studies, which are more sensitive to environmental embrittlement, do suggest a possible embrittlement problem for engineering  $\gamma$  alloys. An order-of-magnitude higher fatigue crack growth rate was observed in air, as compared with vacuum, for alloy K-5 and Ti-47Al-1.5Cr-2Nb.<sup>48,49</sup> The worst-case condition for crack growth resistance was found to occur around 600°C.<sup>49</sup> It is not clear whether the higher fatigue crack growth rates observed in air were associated with very near-surface interstitial oxygen/nitrogen embrittlement, TiN/TiAl<sub>2</sub> formation, or some other mechanism. These data suggest that an oxidation-resistant coating may be beneficial for engineering  $\gamma$  alloys for application temperatures below 750–800°C to protect from environmental embrittlement. At temperatures above 750–800°C, oxidation rates are unacceptably high for many long-term applications, and an oxidation-resistant coating will likely be required.

### OXIDATION-RESISTANT COATINGS FOR GAMMA TITANIUM ALUMINIDES

The development of oxidation-resistant coatings for titanium aluminides was recently reviewed by Taniguchi<sup>50</sup> and Streiff.<sup>51</sup> Three general coating alloy approaches have been taken for protecting titanium aluminides: MCrAlY (M = Ni, Fe, Co),<sup>52–56</sup> aluminizing,<sup>57–63</sup> and silicides/ceramics.<sup>63–66</sup> Protection of titanium aluminides under oxidizing con-

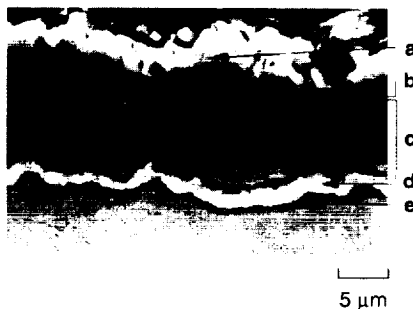


Figure 6. A scanning electron microscopy backscatter-mode micrograph of Ti-48Al-2Cr-2Nb after 9,000 hours at 704°C in air.<sup>40</sup> Note that the identification of TiN and TiAl<sub>2</sub> at the metal/scale interface was based solely on microprobe composition analysis: (a) TiO<sub>2</sub> (light), (b) Al<sub>2</sub>O<sub>3</sub>-rich (dark), (c) intermixed Al<sub>2</sub>O<sub>3</sub> + TiO<sub>2</sub>, (d) TiN, and (e) TiAl<sub>2</sub>.

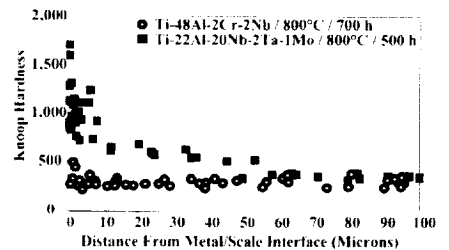


Figure 7. Knoop microhardness data (at 25 g/15 s) as a function of distance from the metal/scale interface for Ti-48Al-2Cr-2Nb and Ti-22Al-20Nb-2Ta-1Mo after 700 hours and 500 hours exposures, respectively, at 800°C in air.<sup>41,47</sup>

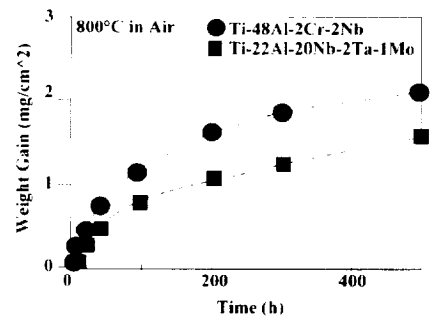


Figure 8. Interrupted weight gain oxidation data for Ti-48Al-2Cr-2Nb and Ti-22Al-20Nb-2Ta-1Mo at 800°C in air.<sup>41,47</sup>

ditions has been achieved with all three approaches, however, studies of such coatings on  $\alpha_2$ - and orthorhombic-based titanium aluminides (monolithic and composite) report severe lifetime degradation under fatigue conditions.<sup>65,67</sup> The fatigue life of coated material is often reduced to below that of uncoated material.<sup>65,67</sup> Similar results are also expected for such coatings that are on  $\gamma$  titanium aluminides.

The degradation in the fatigue life of titanium aluminides by coatings results from three main factors: the formation of brittle coating-substrate reaction zones (chemical incompatibility), the brittleness of the coating alloy, and the differences in the coefficient of thermal expansion between the coating and the substrate (CTE mismatch). MCrAlY coatings, which are successfully used to protect nickel-, iron-, and cobalt-based superalloys, are not chemically compatible with titanium aluminides<sup>54,56</sup> and form brittle coating/substrate reaction zones at 800°C.<sup>54,67</sup> Aluminizing treatments result in the surface formation of the TiAl<sub>3</sub> and TiAl phases, which are brittle and exhibit CTE mismatches with  $\alpha_2$ , orthorhombic, and  $\gamma$  titanium aluminides.<sup>61</sup> Silicide and ceramic coatings are also generally too brittle to survive fatigue conditions.<sup>65,67</sup>

It should be noted that most work to date on the fatigue behavior of coated titanium aluminides has been performed under low-cycle fatigue (LCF) conditions, primarily on  $\alpha_2$ - and orthorhombic-based titanium aluminides. The initial commercial introduction of  $\gamma$  tita-

nium aluminides will likely involve very low load, stiffness-limited applications where less severe high-cycle fatigue (HCF) conditions dominate. Under such conditions, coating alloy property requirements are not as stringent, and it is possible that some of the aforementioned coating approaches may be successful in these cases.

### Ti-Al-Cr Oxidation-Resistant Coating Alloys

The ideal oxidation-resistant coating for  $\gamma$  alloys would be Ti-Al based for optimal chemical and mechanical compatibility with  $\gamma$  substrates, be capable of forming a continuous  $\text{Al}_2\text{O}_3$  scale to protect from both oxidation and interstitial oxygen/nitrogen embrittlement, and possess reasonable mechanical properties to survive HCF. No ideal combination of these properties exists at present. However, reasonable compromises have been achieved with coating alloys based in the Ti-Al-Cr system.

Perkins and Meier et al.<sup>68</sup> discovered that Ti-Al-Cr alloys containing a minimum of 8–10% chromium are continuous  $\text{Al}_2\text{O}_3$  scale formers from 800–1,300°C in air (Figure 9). In a cooperative effort between the University of Pittsburgh (Pitt), Lockheed Missiles and Space Company (LMSC), and General Electric Aircraft Engines (GEAE), the  $\text{Al}_2\text{O}_3$ -forming Ti-Al-Cr alloys were investigated as oxidation-resistant coating alloys for  $\gamma$  titanium aluminides.<sup>69,70</sup> This program met with considerable success. A sputtered Ti-44Al-28Cr coating successfully

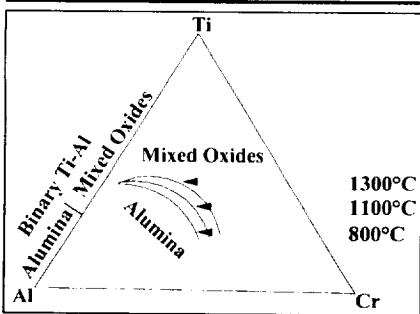


Figure 9. Schematic Ti-Al-Cr oxide map of Perkins and Meier et al.<sup>68</sup>

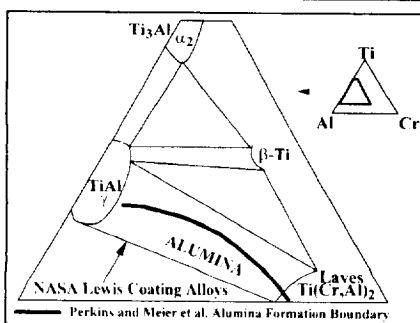


Figure 10. Schematic partial 800–1,000°C Ti-Al-Cr phase diagram,<sup>75</sup> based on References 71–75 and 79, showing the composition range of the  $\gamma$  + Laves NASA Lewis oxidation-resistant coating alloys.<sup>78</sup>

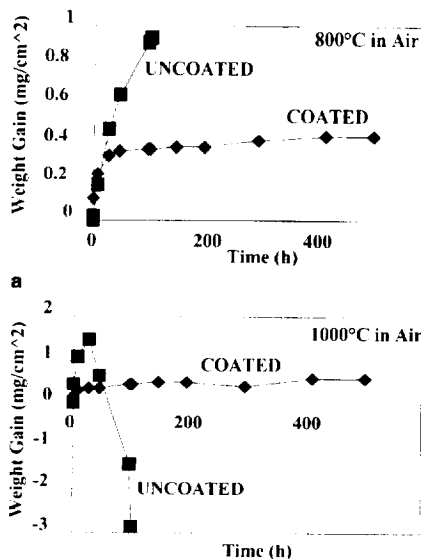


Figure 11. Interrupted weight-gain oxidation data for LPPS Ti-51Al-12Cr-coated and uncoated Ti-48Al-2Cr-2Nb at (a) 800°C and (b) 1,000°C in air.

protected Ti-47Al-2Cr-2Ta under long-term (2,000 hours) cyclic oxidation at 900°C in air.<sup>70</sup> Coating composition optimization studies identified Ti-50Al-20Cr as holding the most promise as an oxidation-resistant coating for  $\gamma$  alloys.<sup>69</sup> However, the Ti-Al-Cr alloys examined under this program were brittle and exhibited some minor chemical incompatibility problems (e.g., small reaction zone of chromium-rich precipitates) with  $\gamma$  alloy substrates.<sup>69</sup> Difficulties in depositing high-quality coatings by plasma spray methods were also encountered.<sup>69</sup>

A second generation of Ti-Al-Cr coating alloys based on the Pitt/LMSC/GEAE work was recently developed at the NASA Lewis Research Center. The goal of this program was to co-optimize the oxidation resistance, mechanical properties, and  $\gamma$  alloy compatibility of Ti-Al-Cr coating alloys. To accomplish this, the critical phase equilibria in the  $\text{Al}_2\text{O}_3$ -forming composition range were determined,<sup>71</sup> and a microstructure/property approach was adopted.<sup>72</sup>

The  $\text{Al}_2\text{O}_3$ -forming Ti-Al-Cr composition range was found to be multiphase and consisted primarily of the  $\tau$  ( $\text{L}_2$  phase centered on Ti-67Al-8Cr) or  $\gamma$  phases and the  $\text{Ti}(\text{Cr},\text{Al})_2$  (Laves<sup>73,74</sup>) phase.<sup>71</sup> The key to oxidation resistance was the Laves phase, which was capable of continuous  $\text{Al}_2\text{O}_3$  scale formation despite an aluminum content of only 37–42%.<sup>72,75</sup> Unfortunately, the Laves phase was also a major source of alloy brittleness.<sup>72</sup>

Work by Klansky et al. on Ti-Al-Cr alloys hot isostatically pressed at 1,200°C showed that mixing the Laves phase with the  $\tau$  phase or the  $\gamma$  phase improved cracking resistance (i.e., reduced alloy brittleness) as measured by room-temperature microhardness indentation.<sup>73</sup>

Their results suggest that basing a Ti-Al-Cr coating alloy on either the  $\tau$  phase or the  $\gamma$  phase would reduce alloy brittleness; however, the  $\tau$  phase in this composition range decomposes to the brittle  $\text{TiAl}_3$  phase and a chromium-rich phase ( $\text{Cr}_2\text{Al}^{71}$  or, more likely,  $\beta\text{-Cr}^{76}$ ) on exposure at 800°C. Thus, any beneficial effects of the  $\tau$  phase on cracking resistance are lost after exposure in the temperature range where application of these coating alloys is expected.<sup>71</sup>

In contrast, the  $\gamma$  phase in the  $\text{Al}_2\text{O}_3$ -forming Ti-Al-Cr alloys is stable from room temperature to at least 1,000°C.<sup>71,72</sup> Additionally, the  $\gamma$  phase is capable of some limited room-temperature ductility.<sup>77</sup> Therefore, the best current option for reducing Ti-Al-Cr coating alloy brittleness is to base the alloy on the  $\gamma$  phase.<sup>71,72</sup> Most of the Pitt/LMSC/GEAE coating alloys were based on the Laves phase (Ti-44Al-28Cr) or the  $\tau$  phase (Ti-50Al-20Cr).

A region of  $\text{Al}_2\text{O}_3$ -forming  $\gamma$  + Laves Ti-Al-Cr coating alloys was identified by Brady et al.,<sup>78</sup> in which the  $\gamma$  phase was continuous in the microstructure (Figure 10). This further reduces brittleness because the brittle Laves phase is surrounded by the  $\gamma$  phase in the microstructure. Compatibility with  $\gamma$  alloys is also optimized because these Ti-Al-Cr coating alloys consist predominately of the  $\gamma$  phase.

A representative  $\gamma$  + Laves coating alloy, Ti-51Al-12Cr,<sup>78</sup> was applied to Ti-48Al-2Cr-2Nb by low-pressure plasma spray (LPPS). Interrupted weight-gain oxidation tests at 800°C and 1,000°C in air indicated that the coating successfully protected the substrate from oxidation (Figure 11). A typical coating/substrate region after 100 hours at 1,000°C in air is shown in Figure 12. The absence of a significant interdiffusion zone with the substrate demonstrate the excellent chemical and thermal compatibility of the Ti-51Al-12Cr coating with the Ti-48Al-2Cr-2Nb substrate.

A high-magnification micrograph of

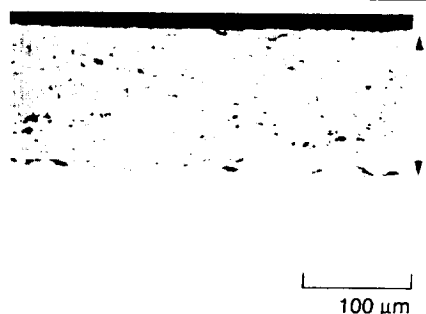


Figure 12. A scanning electron microscopy backscatter-mode micrograph of LPPS Ti-51Al-12Cr-coated Ti-48Al-2Cr-2Nb after 100 hours of interrupted weight gain exposure at 1,000°C in air. The coating area is indicated by the range marker. The black areas in the coating are porosity.



Figure 13. A scanning electron microscopy backscatter-mode micrograph of an LPPS Ti-51Al-12Cr coating after 500 hours of interrupted weight-gain exposure at 1,000°C in air. The microstructure consists of the  $\gamma$  phase (dark) and the Laves phase (light). The black regions are porosity. The Vicker's microhardness indentation was performed at 1 kg for 15 seconds.

the LPPS Ti-51Al-12Cr coating after exposure at 1,000°C for 500 hours is shown in Figure 13. In general, the Laves phase regions in the microstructure are surrounded by the  $\gamma$  phase. The crack resistance imparted to the coating alloy by the continuous  $\gamma$  phase microstructure was evaluated via microhardness indent evaluation. Under 1 kg/15 s indentation conditions, only small isolated cracks 1–3  $\mu\text{m}$  in length were observed (Figure 13). The cracks were confined to the Laves phase and were blunted at the Laves/ $\gamma$  interface. At lower loads, no cracking was observed. In contrast, Laves-based alloys suffer from extensive cracking after microhardness indentation at loads of only 100 g.<sup>72</sup> Evaluation of the LCF and HCF behavior of LPPS Ti-51Al-12Cr-coated Ti-48Al-2Cr-2Nb is in progress.

## CONCLUSION

In terms of environmental durability (oxidation and interstitial embrittlement), the  $\gamma$  class of titanium aluminides looks promising for applications below 750–800°C in air. Future work should emphasize the interaction between environmental effects and mechanical properties, fatigue, in particular. For applications above 750–800°C, an oxidation-resistant coating will likely be necessary for  $\gamma$  alloys. Future coating alloy development should include an evaluation of the effects of the coating on fatigue life.

## ACKNOWLEDGEMENTS

The authors thank Sushil Jain of Allison Engine Company, Jon Schaeffer of GEAE, and Young-Won Kim of Universal Energy Systems for providing gamma material for study and for their helpful discussions. The authors also thank J. Nesbitt, J. Doychak, F. Dettenwanger, and B. Gleeson for their helpful discussions. M.P. Brady acknowledges the financial support of a National Research Council post-doctoral fellowship. The NASA

Lewis Ti-Al-Cr coating alloy development program was funded under the Advanced High Temperature Engine Materials Technology Program (HITEMP).

## References

1. Y.W. Kim and F.H. Froes, *High Temperature Aluminides and Intermetallics*, ed. S.H. Whang et al. (Warrendale, PA: TMS, 1990), p. 465.
2. M. Yamaguchi, *Titanium '92*, ed. F.H. Froes and I. Caplan (Warrendale, PA: TMS, 1993), p. 959.
3. S.-C. Huang, U.S. patent 4,879,092 (1989).
4. U.R. Kattner, J.-C. Lin, and Y.A. Chang, *Met. Trans. A*, 23A (1992), p. 2081.
5. G.H. Meier et al., *Oxidation of High Temperature Intermetallics*, ed. T. Grobstein and J. Doychak (Warrendale, PA: TMS, 1988), p. 185.
6. S. Becker et al., *Ox. Met.*, 38 (5/6) (1992), p. 425.
7. K. Maki et al., *Mat. Sci. and Eng.*, A153 (1992), p. 591.
8. S.A. Kekare, D.K. Shelton, and P. B. Aswath, *Mat. Res. Soc. Symp. Proc.*, vol. 288 (Pittsburgh, PA: MRS, 1993), p. 1025.
9. Y. Shida and H. Anada, *Mat. Trans. JIM*, 35 (9) (1994), p. 623.
10. A. Rahmel, W.J. Quadackers, and M. Schutze, *Materials and Corrosion*, 46 (1995), p. 281.
11. V.V. Samokhval, P.A. Poleshuk, and A.A. Vecher, *Russ. J. Phys. Chem.*, 45 (8) (1971), p. 1174.
12. M. Hoch and R.J. Usell, Jr., *Met. Trans.*, 2 (1971), p. 2627.
13. N.S. Jacobson, M.P. Brady, and G.M. Mehrotra, "Twin Knudsen Cell Measurements of Aluminum Activities in TiAl Alloys," *Electrochemical Society Extended Abstracts, 188th Meeting of the Electrochemical Society* (Pennington, NJ: the Electrochemical Society, 1995).
14. M. Eckert et al., *Ber. Bunsenges. Phys. Chem.*, 100 (4) (1996), p. 418.
15. K.L. Luthra, *Ox. Met.*, 36 (5/6) (1991), p. 475.
16. A. Rahmel and P.J. Spencer, *Ox. Met.*, 35 (1/2) (1991), p. 53.
17. X.L. Li et al., *Acta Metall. Mater.*, 40 (11) (1992), p. 3149.
18. M.-X. Zhang et al., *Scripta Met. Mater.*, 27 (1992), p. 1361.
19. G.P. Kelkar and A.H. Carim, *J. Am. Ceram. Soc.*, 78 (3) (1995), p. 572.
20. Y. Chen, D.J. Young, and B. Gleeson, *Materials Letters*, 22 (1995), p. 125.
21. W.E. Dowling, Jr. and W.T. Donlon, *Scripta Met. et Mater.*, 27 (1992), p. 1663.
22. R.W. Beyer and R. Gronsky, *Acta Met. et Mater.*, 42 (1994), p. 1373.
23. N. Zheng et al., *Scripta Met. et Mater.*, 33 (1995), p. 47.
24. Y.F. Cheng et al., *Scripta Materialia*, 34 (5) (1996), p. 707.
25. F. Dettenwanger et al., "Development and Microstructure of the Al-Depleted Layer of Oxidized TiAl," *Materials and Corrosion*, in press.
26. E.H. Copland, B. Gleeson, and D.J. Young, "Factors Affecting the Sub-Surface Formation of a Ti<sub>3</sub>Al<sub>2</sub>O<sub>5</sub> Phase During Oxidation of  $\gamma$ -TiAl Based Alloys," *Proceedings of the 13th International Corrosion Congress* (Melbourne, Australia: Int. Cor. Council, 1996).
27. N.S. Choudhury, H.C. Graham, and J.W. Hinze, *Properties of High Temperature Alloys*, ed. Z.A. Fouroulis and F.S. Pettit (Pennington, NJ: the Electrochemical Society, 1976), p. 668.
28. F. Dettenwanger et al., *Mat. Res. Soc. Symp.*, vol. 364 (1995), p. 981.
29. J.M. Rakowski et al., *Scripta Met. et Mater.*, 33 (1995), p. 997.
30. N. Zheng et al., *Ox. Met.*, 44 (5/6) (1995), p. 477.
31. R.A. Perkins, K.T. Chiang, and G.H. Meier, *Scripta Met.*, 21 (1987), p. 1505.
32. T.A. Wallace et al., *Environmental Effects on Advanced Materials*, ed. R.H. Jones and R.E. Ricker (Warrendale, PA: TMS, 1991), p. 79.
33. Y.-W. Kim, *Mat. Res. Soc. Symp. Proc.*, vol. 213 (Pittsburgh, PA: MRS, 1991), p. 777.
34. D.W. McKee and S.C. Huang, *Corrosion Science*, 33 (12) (1992), p. 1899.
35. B.C. Kim, G.M. Kim, and C.J. Kim, *Scripta Met. et Mater.*, 33 (7) (1995), p. 1117.
36. J. Doychak, *Intermetallic Compounds*, ed. J.H. Westbrook and R.L. Fleischer (New York: John Wiley & Sons Ltd, 1994), p. 977.
37. J.C. Schaeffer, C.M. Austin, and F. Kaempf, *Gamma Titanium Aluminides*, ed. Y.-W. Kim, R. Wagner, and M. Yamaguchi (Warrendale, PA: TMS, 1995), p. 71.
38. M. Yoshihara, K. Miura, and Y.-W. Kim, *Gamma Titanium Aluminides*, ed. Y.-W. Kim, R. Wagner, and M. Yamaguchi (Warrendale, PA: TMS, 1995), p. 93.
39. Y. Shida and H. Anada, *Ox. Met.*, 45 (1/2) (1996), p. 197.
40. I.E. Locci et al., "Very Long Term Oxidation of Ti-48Al-2Cr-2Nb at 704°C in Air," submitted to *Scripta Mater.*
41. W.J. Brindley, unpublished research.
42. Y.-W. Kim, *JOM*, 46 (7) (1994), p. 30.
43. S. Jain and J.R. Roessler, U.S. patent 5,296,056 (1994).
44. M. Schutze and M. Schmitz-Niederer, *Gamma Titanium Aluminides*, ed. Y.-W. Kim, R. Wagner, and M. Yamaguchi (Warrendale, PA: TMS, 1995), p. 83.
45. J.L. Smialek et al., *Mat. Res. Soc. Symp.*, vol. 364 (1995), p. 1273 (1995).
46. G.H. Meier, "Research on Oxidation and Embrittlement of Intermetallic Compounds in the U.S.," to be published in *Materials and Corrosion*.
47. W.J. Brindley et al., *HITEMP Review-1994*, NASA CP-10146, vol. II, paper 44 (1994).
48. A.H. Rosenberger, B.D. Worth, and S.J. Balsone, "Environmental Effects on the Fatigue Crack Growth of Gamma Titanium Aluminides," to be published in the proceedings of

- Sixth International Fatigue Congress, Berlin (May, 1996).
49. S.J. Balsone et al., *Mat. Sci. and Eng.*, A192/193 (1995), p. 457.
50. S. Taniguchi, *MRS Bulletin* (October 1994), p. 31.
51. R. Streiff, *Journal De Physique IV, Colloque C9*, vol. 3 (1993), p. 17.
52. T. Shimizu, T. Ikubo, and S. Isobe, *Mat. Sci. and Eng.*, A153 (1992), p. 602.
53. W.J. Brindley, J.L. Smialek, and C.J. Rouge, U.S. patent 5,116,690 (1992).
54. W.J. Brindley, J.L. Smialek, and M.A. Gedwill, *HITEMP Review-1992*, NASA CP-10104, vol. II, paper 41 (1992).
55. D.W. McKee, *Mat. Res. Soc. Proc.*, 288 (1993), p. 953.
56. D.W. McKee and K.L. Luthra, *Surface and Coatings Technology*, 56 (1993), p. 109.
57. R. Streiff and S. Poize, *High Temperature Corrosion*, ed. R.A. Rapp (Houston, TX: NACE, 1983), p. 591.
58. H. Mabuchi, T. Asai, and Y. Nakayama, *Scripta Met.*, 23 (1989), p. 685.
59. J.L. Smialek, M.A. Gedwill, and P.K. Brindley, *Scripta Met. et Mater.*, 24 (1990), p. 1291.
60. M. Yoshihara, T. Suzuki, and R. Tanaka, *ISIJ International*, 31 (10) (1991), p. 1201.
61. J.L. Smialek, *Corrosion Science*, 35 (5-8) (1993), p. 1199.
62. C. Levys, M. Peters, and W.A. Kaysser, "Influence of Intermetallic Ti-Al Coatings on the Creep Properties of Timetal 1100," submitted to *Scripta Mater.*
63. T.C. Munro and B. Gleeson, "The Deposition of Aluminide and Silicide Coatings on  $\gamma$ -TiAl Using the Halide-Activated Pack Cementation Method," *Met. Mat. Trans.*, in press.
64. R.P. Skowronski, *J. Am. Ceram. Soc.*, 77 (4) (1994), p. 1098.
65. W.C. Revelos and P.R. Smith, *Met. Trans. A*, 23A (1992), p. 587.
66. B. Cockeram and R.A. Rapp, *Ox. Met.*, 45 (5/6) (1996), p. 427.
67. W.J. Brindley and P.A. Bartolotta, unpublished research.
68. R.A. Perkins and G.H. Meier, *Proceedings of the Industry-University Advanced Materials Conference II*, ed. F. Smith (Golden, CO: Advanced Materials Institute, 1989), p. 92.
69. J.C. Schaeffer et al., GE Aircraft Engines final report, Naval Air Development Center contract N62269-90-F-C-0287 (1993).
70. R.L. McCarron et al., *Titanium 1992*, ed. F.H. Froes and I. Caplan (Warrendale, PA: TMS, 1993), p. 1971.
71. M.P. Brady, J.L. Smialek, and F. Terepka, *Scripta Met. Mater.*, 32 (10) (1995), p. 1659.
72. M.P. Brady, J.L. Smialek, and D.L. Humphrey, *Mat. Res. Soc. Symp.*, vol. 364 (1995), p. 1309.
73. J.L. Klansky, J.P. Nic, and D.E. Mikkola, *J. Mater. Res.*, 9 (1994), p. 255.
74. T.J. Jewett and M. Dahms, *Z. Metallkunde*, 87 (1996).
75. M.P. Brady et al., "The Role of Cr in Promoting Protective Alumina Scale Formation by  $\gamma$ -Based Ti-Al-Cr Alloys: Part I: Compatibility with Alumina and Oxidation Behavior in Oxygen," to be published in *Acta Met.*
76. T.J. Jewett, B. Ahrens, and M. Dahms, "Phase Equilibria Involving the  $\gamma$ -Ti, and TiAl, Phases in the Ti-Al-Cr System," *Intermetallics*, in press.
77. S.-C. Huang and E.L. Hall, *Met. Trans. A*, 22A (1991), p. 2619.
78. M.P. Brady, J.L. Smialek, and W.J. Brindley, submitted to U.S. patent office (1996).
79. F.H. Hayes, *J. Phase Equilibria*, 13 (1) (1992), p. 79.

## ABOUT THE AUTHORS

**Michael P. Brady** earned his Ph.D. in materials science and engineering from the University of Florida in 1993. He is currently a National Research Council post-doctoral fellow with NASA Lewis Research Center in Cleveland, Ohio. He is also a member of TMS.

**William J. Brindley** his Ph.D. in metallurgical engineering from Michigan Technological University in 1986. His is currently a research scientist with NASA Lewis Research Center in Cleveland, Ohio.

**James L. Smialek** earned his Ph.D. in materials science from Case Western Reserve University in 1981. His is currently a senior research scientist with NASA Lewis Research Center in Cleveland, Ohio. He is also a member of TMS.

**Ivan E. Locci** earned his Ph.D. in materials science from Case Western Reserve University in 1986. He is currently a principal researcher at Case Western Reserve University in Cleveland, Ohio, and a research associate with NASA Lewis. He is also a member of TMS.

For more information, contact M.P. Brady, NASA Lewis Research Center, MS 106-1, 21000 Brook Park Road, Cleveland, Ohio 44135; (216) 433-5504; fax (216) 433-5544; e-mail MichaelP.Brady@lerc.nasa.gov.